Friction Models and Friction Compensation

H. Olsson[†] **K.J. Åström**[†] **C. Canudas de Wit**[‡]
M. Gäfvert[†] **P. Lischinsky**[††]

Abstract

1. Introduction

Friction occurs in all mechanical systems,e.g. bearings, transmissions, hydraulic and pneumatic cylinders, valves, brakes and wheels. Friction appears at the physical interface between two surfaces in contact. Lubricants such as grease or oil are often used but the there may also be a dry contact between the surfaces. Friction is strongly influenced by contaminations. There is a wide range of physical phenomena that cause friction, this includes elastic and plastic deformations, fluid mechanics and wave phenomena, and material sciences, see [45, 53, 9, 10].

Friction was studied extensively in classical mechanical engineering and there has lately been a strong resurgence. Apart from intellectual curiosity this is driven by strong engineering needs in a wide range of industries from disc drives to cars. The availability of new precise measurement techniques has been a good driving force.

Friction is also very important for the control engineer, for example in design of drive systems, high-precision servo mechanisms, robots, pneumatic and hydraulic systems and anti-lock brakes for cars. Friction is highly nonlinear and

[†] Department of Automatic Control, Lund Institute of Technology, Lund University, Box 118, S-221 00 LUND, Sweden
[‡] Laboratoire d'Automatique de Grenoble, CNRS-INPG-UJF, ENSIEG-INPG, B.P. 46, 38402 Grenoble, France
[††] Control Department, EIS, ULA, Mérida 5101, Venezuela

may result in steady state errors, limit cycles, and poor performance. It is therefore important for control engineers to understand friction phenomena and to know how to deal with them. With the computational power available today it is in many cases possible to deal effectively with friction. This has potential to improve quality, economy, and safety of a system.

Friction should be considered early in the system design by reducing it as much as possible through good hardware design. There are, however, cost constraints that may be prohibitive. Dither is a simple way to reduce static friction that has been used for a long time. Dither can be introduced electronically or mechanically by a vibrator, as was done in early auto pilots, see [41]. Recent advances in computer control have also shown the possibility to reduce the effects of friction by estimation and control. There has also been a significantly increased interest in friction in the control community in terms of special sessions at conferences and papers, see [], [].

It is useful for the control engineer to understand friction so well that he, or she, can understand the effects of friction on a closed loop, and design control laws that reduce the effects of friction. The goal of this paper is to contribute to such knowledge. The paper is organized as follows. A brief description of friction phenomena is given in Section 2. A number of friction models are described. The models all attempt to capture the essence of the complicated friction phenomena with models of reasonable complexity. The nature of the models are quite different. They can be static or dynamic. They can be described by differential equations, differential algebraic equations or hybrid models that include events. Static models are surveyed in Section 3 and dynamic models in Section 4. In Section 5 we compare the behavior of two models in typical control situations. Section 6 compares the behavior of some models for small displacements, which is of particular interest for control, and in Section 7 we discuss some application of the models to typical control problems such as friction observers and friction compensation.

2. Friction phenomena

Friction is the tangential reaction force between two surfaces in contact. Physically these reaction forces are the results of many different mechanisms, which depend on contact geometry and topology, properties of the bulk and surface materials of the bodies, displacement and relative velocity of the bodies and

presence of lubrication.

In dry sliding contacts between flat surfaces friction can be modeled as elastic and plastic deformation forces of microscopical asperities in contact, see [9, 10]. The asperities each carry a part f_i of the normal load F_N. If we assume plastic deformation of the asperities until the contact area of each junction has grown large enough to carry its part of the normal load, the contact area of each asperity junction is $a_i = f_i/H$, where H is the hardness of the weakest bulk material of the bodies in contact. The total contact area can thus be written $A_r = F_N/H$. This relation holds even with elastic junction area growth, provided that H is adjusted properly. For each asperity contact the tangential deformation is elastic until the applied shear pressure exceeds the shear strength τ_y of the surface materials, when it becomes plastic. In sliding the friction force thus is $F_T = \tau_y A_R$, and the friction coefficient $\mu = F_T/F_N = \tau_y/H$. The friction coefficient is not dependent on the normal load or the velocity in this case. Consequently it is possible to manipulate friction characteristics by deploying surface films of suitable materials on the bodies in contact. These surface films can also be the result of contaminations or oxidation of the bulk material.

In dry rolling contact, friction is the result of a non-symmetric pressure distribution in the contact. The pressure distribution is caused by elastic hysteresis in either of the bodies, or local sliding in the contact. For rolling friction the friction coefficient is proportional to the normal load as $\mu \propto F_N^a$, with $0.2 < a < 1.4$.

The elasto-plastic characteristics of dry friction can be described by hysteresis theory, see [54].

Other physical mechanisms appear when lubrication is added to the contact. For low velocities, the lubricant acts as a surface film, where the shear strength determines the friction. At higher velocities at low pressures a fluid layer of lubricant is built up in the surface due to hydrodynamic effects. Friction is then determined by shear forces in the fluid layer. These shear forces depend on the viscous character of the lubricant, as well as the shear velocity distribution in the fluid film. Approximate expressions for the friction coefficient exist for a number of contact geometries and fluids. At high velocities and pressures the lubricant layer is built up by elasto-hydrodynamic effects. In these contacts the lubricant is transformed into an amorphous solid phase due to the high pressure. The shear forces of this solid phase turns out to be practically independent of the shear velocity.

The shear strength of a solid lubricant film at low velocities is generally higher than the shear forces of the corresponding fluid film built up at higher velocities. As a result the friction coefficient in lubricated systems normally de-

creases when the velocity increases from zero. When the thickness of the film is large enough to completely separate the bodies in contact, the friction coefficient may increase with velocity as hydrodynamic effects becomes significant. This is called the Stribeck effect.

Film thickness is a vital parameter in lubricated friction. The mechanisms underlying the construction of the fluid film includes dynamics, thus suggesting a dynamic friction model.

Contamination is another factor that adds complication. The presence of small particles of different material between the surfaces give rise to additional forces that strongly depend on the size and material properties of the contaminants.

This short expose of some friction mechanisms illustrate the difficulty in modeling friction. There are many different mechanisms. To construct a general friction model from physical first principles is simply not possible. Approximate models exist for certain configurations. What we look for instead is a general friction model for control applications, including friction phenomena observed in those systems.

The behavior of friction has been extensively examined during the 20th century. The experiments have been performed under idealized conditions with clean surfaces and for stationary conditions, e.g., constant velocity. Lately the interest in friction dynamics has increased. Some experimental observations of friction are reviewed below. The collection is by no means complete but serves to illustrate the many facets of friction behavior.

Steady Velocity Friction

The friction force as a function of velocity for constant velocity motion is called the Stribeck curve after the work of Stribeck in [52]. In particular the dip in the force at low velocities is called the Stribeck effect, see Figure 5. The friction-velocity relation is application dependent and varies with material properties, temperature, wear etc. Many friction phenomena do not appear for constant velocity experiments. A number of observations of the dynamic behavior are given in the following.

Static Friction and Break-Away Force

Static friction is the friction when sticking. The force required to overcome the static friction and initiate motion is called the break-away force. Many experimental investigations were performed in the 50s to study the nature of static friction and the break-away force.

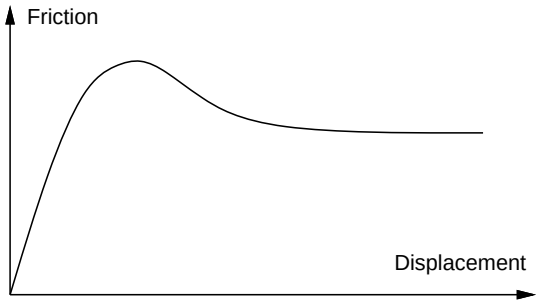

Figure 1 The relation between friction and displacement as found by [44]. The experimental results suggested that friction should be described as a function of displacement and not velocity.

Rabinowicz addressed the transition between sticking and sliding in [44]. He investigated friction as a function of displacement. He concluded that the break-away force is given by the peak seen in Figure 1. The maximum friction force typically occurs at a small displacement from the starting point. In [33] it was found experimentally that the break-away force depends on the rate of increase of the external force. This is confirmed in [48]. A characteristic behavior is shown in Figure 2. Another investigation of the behavior in the sticking regime was done by [16]. They studied the spring-like behavior before gross sliding occurs. Their results were presented in diagrams showing force as a function of displacement, see Figure 3. Note the differences between Figures 1 and 3. The microscopic motion is often called pre-sliding motion.

Frictional Lag

That dynamics are not only important when sticking was shown by Hess and Soom in the paper [31]. They performed experiments with a periodic time-varying velocity superimposed on a bias velocity so that the motion becomes unidirectional. Typically the friction–velocity relation appeared as in Figure 4. Hysteresis

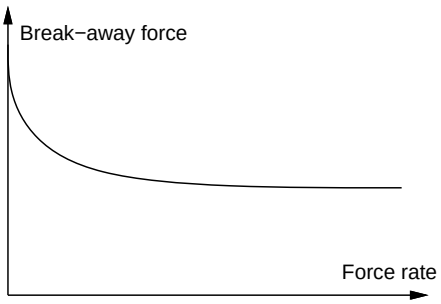

Figure 2 Characteristic relation between rate of force application and break-away force as found in [33]. The experiment suggested that the break-away force decreases with increased rate of force application.

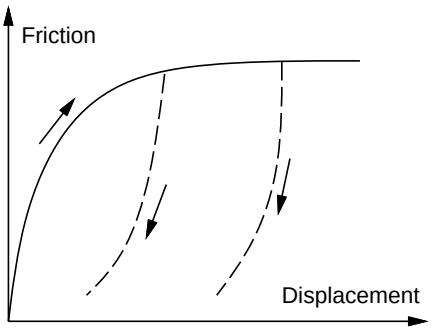

Figure 3 Pre-Sliding displacement as found by [16]. The result agrees with Figure 1 for small displacements. Releasing the applied force results in a permanent displacement as indicated by the dashed lines.

was observed as the velocity varied. The size of the loop increased with normal load, viscosity and frequency of the velocity variation.

These experiments clearly indicate the necessity of using dynamic friction models.

3. Static models

In this section we will give a brief summary of some static friction models.

Classical Models

The classical models of friction consist of different components, which each take care of certain aspects of the friction force. The main idea is that friction opposes motion and that its magnitude is independent of velocity and contact area. It can therefore be described as

$$F = F_C \operatorname{sgn}(v), \tag{1}$$

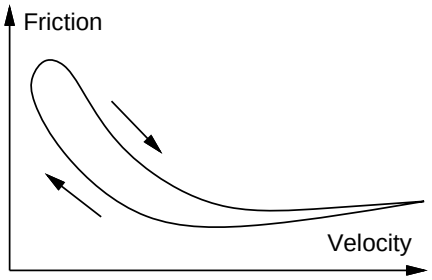

Figure 4 The friction–velocity relation observed in [31]. The friction force is lower for decreasing velocities than for increasing velocities. The hysteresis loop becomes wider as the velocity variations become faster.

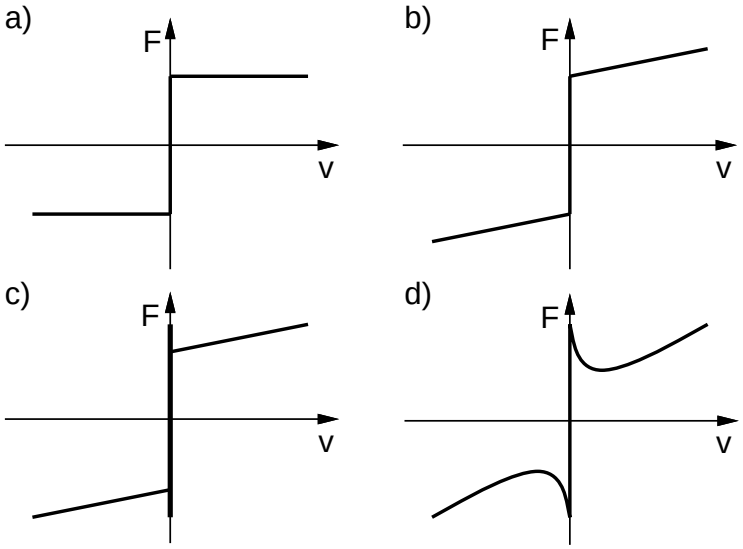

Figure 5 Examples of static friction models. The friction force is given by a static function except possibly for zero velocity. Figure **a)** shows Coulomb friction and Figure **b)** Coulomb plus viscous friction. Stiction plus Coulomb and viscous friction is shown in Figure **c)** and Figure **d)** shows how the friction force may decrease continuously from the static friction level.

where the friction force F_C is proportional to the normal load, i.e. $F_C = \mu F_N$. This description of friction is termed *Coulomb friction*, see Figure 5 a). Notice that the model (1) is an ideal relay model. The Coulomb friction model does not specify the friction force for zero velocity. It may be zero or it can take on any value in the interval between $-F_C$ and F_C, depending on how the sign function is defined. The Coulomb friction model has, because of its simplicity, often been used for friction compensation, see [24, 4].

In the 19th century the theory of hydrodynamics was developed leading to expressions for the friction force caused by the viscosity of lubricants, see [47]. The term *viscous friction* is used for this force component, which is normally described as

$$F = F_v v \tag{2}$$

Viscous friction is often combined with Coulomb friction as shown in Figure 5 b). Better fit to experimental data can often be obtained by a nonlinear dependence on velocity, e.g.

$$F = F_v |v|^{\delta_v} \operatorname{sgn}(v) \tag{3}$$

where δ_v depends on the geometry of the application, see [50] and [1].

Stiction is short for static friction as opposed to dynamic friction. It describes the friction force at rest. [37] introduced the idea of a friction force at rest that is higher than the Coulomb friction level. Static friction counteracts external forces below a certain level and thus keeps an object from moving.

It is hence clear that friction at rest cannot be described as a function of only velocity. Instead it has to be modeled using the external force F_e in the following manner.

$$F = \begin{cases} F_e & \text{if } v = 0 \text{ and } |F_e| < F_S \\ F_S \operatorname{sgn}(F_e) & \text{if } v = 0 \text{ and } |F_e| \geq F_S \end{cases} \tag{4}$$

The friction force for zero velocity is a function of the external force and not the velocity. The traditional way of depicting friction in block diagrams with velocity as the input and force as the output is therefore not completely correct. If doing so, stiction must be expressed as a multi-valued function that can take on any value between the two extremes $-F_S$ and F_S. Specifying stiction in this way leads to non-uniqueness of the solutions to the equations of motion for the system, see [8].

The classical friction components can be combined in different ways, see Figure 5 c), and any such combination is referred to as a classical model. These models have components that are either linear in velocity or constant. Stribeck observed in [52] that the friction force does not decrease discontinuously as in Figure 5 c), but that the velocity dependence is continuous as shown in Figure 5 d). This is called Stribeck friction. A more general description of friction than the classical models is, therefore,

$$F = \begin{cases} F(v) & \text{if } v \neq 0 \\ F_e & \text{if } v = 0 \text{ and } |F_e| < F_S \\ F_S \operatorname{sgn}(F_e) & \text{otherwise} \end{cases} \tag{5}$$

where $F(v)$ is an arbitrary function, which may look as in Figure 5 d). A number of parameterizations of $F(v)$ have been proposed, see [2]. A common form of the nonlinearity is

$$F(v) = F_C + (F_S - F_C)e^{-|v/v_S|^{\delta_S}} + F_v v \tag{6}$$

where v_S is called the Stribeck velocity. Such models have been used for a long time. The function F is easily obtained by measuring the friction force for motions with constant velocity. The curve is often asymmetrical.

The Karnopp Model

The main disadvantage when using a model such as (5), for simulations or control purposes, is the problem of detecting when the velocity is zero. A remedy for this is found in the model presented by Karnopp in [34]. It was developed to overcome the problems with zero velocity detection and to avoid switching between different state equations for sticking and sliding. The model defines a zero velocity interval, $|v| < DV$. For velocities within this interval the internal state of the system (the velocity) may change and be non-zero but the output of the block is maintained at zero by a dead-zone. Depending on if $|v| < DV$ or not, the friction force is either a saturated version of the external force or an arbitrary static function of velocity. The interval $\pm DV$ can be quite coarse and still promote so called stick-slip behavior.

The drawback with the model is that it is so strongly coupled with the rest of the system. The external force is an input to the model and this force is not always explicitly given. The model therefore has to be tailored for each configuration. Variations of the Karnopp model are widely used since they allow efficient simulations. The zero velocity interval does, however, not agree with real friction.

The friction models presented so far have considered friction only for steady velocities. No attention is paid to the behavior of friction as the velocity is varied.

Armstrong's Model

To account for some of the observed dynamic friction phenomena a classical model can be modified as proposed by Armstrong in [3]. This model introduces temporal dependencies for stiction and Stribeck effect, but does not handle presliding displacement. This is instead done by describing the sticking behavior by a separate equation. Some mechanism must then govern the switching between the model for sticking and the model for sliding. The friction is described by

$$F(x) = \sigma_0 x \tag{7}$$

when sticking and by

$$F(v,t) = \left(F_C + F_S(\gamma, t_d) \frac{1}{1 + (v(t-\tau_l)/v_S)^2} \right) \operatorname{sgn}(v) + F_v v \tag{8}$$

when sliding, where

$$F_S(\gamma, t_d) = F_{S,a} + (F_{S,\infty} - F_{S,a} \frac{t_d}{t_d + \gamma}) \tag{9}$$

$F_{S,a}$ is the Stribeck friction at the end of the previous sliding period and t_d the dwell time, i.e., the time since becoming stuck. The sliding friction (8) is equivalent to a static model where the momentary value of the velocity in the Stribeck friction has been replaced by a delayed version and where it has a time dependent coefficient. The model requires seven parameters.

Since the model consists of two separate models, one for sticking and one for sliding, a logical statement—probably requiring an eighth parameter—determines the switching. Furthermore, the model states have to be initialized appropriately every time a switch occurs.

4. Dynamic models

Lately there has been a significant interest in dynamic friction models. This has been driven by intellectual curiosity, demands for precision servos and advances in hardware that makes it possible to implement friction compensators. In this section we will present several dynamic models.

The Dahl Model

The Dahl model introduced in [18] was developed for the purpose of simulating control systems with friction. The model is also discussed in [19] and [21], and has also been used for adaptive friction compensation, see [55] and [23]. Dahl's starting point were several experiments on friction in servo systems with ball bearings. One of his findings was that bearing friction behaved very similar to solid friction. These experiments indicate that there are metal contacts between the surfaces. Dahl developed a comparatively simple model that was used extensively to simulate systems with ball bearing friction.

The starting point for Dahl's model is the stress-strain curve in classical solid mechanics, see [46] and [49], and Figure 6. When subject to stress the friction force increases gradually until rupture occurs. Dahl modeled the stress-strain curve by a differential equation. Let x be the displacement, F the friction force, and F_c the Coulomb friction force. Then Dahl's model has the form

$$\frac{dF}{dx} = \sigma\left(1 - \frac{F}{F_c}\operatorname{sgn} v\right)^{\alpha}$$

where σ is the stiffness coefficient and α is a parameter that determines the shape of the stress-strain curve. The value $\alpha = 1$ is most commonly used. Higher

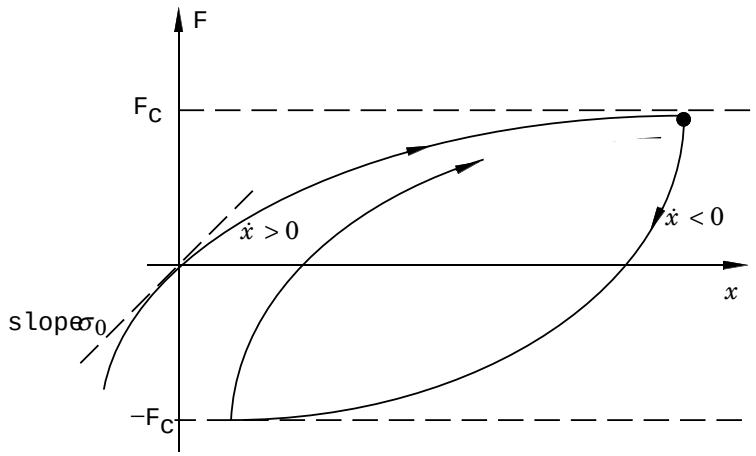

Figure 6 Friction force as a function of displacement for Dahl's model.

values will give a stress strain curve with a sharper bend. The friction force $|F|$ will never be larger than F_c if its initial value is such that $|F(0)| < F_c$.

Notice that in this model the friction force is only a function of the displacement and the sign of the velocity. This implies that the friction force is only position dependent. This so called rate independence is an important property of the model. It makes it possible to use the theory of hysteresis operators [35]. It is also used in extensions of the model, see [5].

To obtain a time domain model Dahl observed that

$$\frac{dF}{dt} = \frac{dF}{dx}\frac{dx}{dt} = \frac{dF}{dx}v = \sigma\left(1 - \frac{F}{F_c}\operatorname{sgn} v\right)^{\alpha} v. \tag{10}$$

The model is a generalization of ordinary Coulomb friction. The Dahl model neither captures the Stribeck effect, which is a rate dependent phenomenon, nor does it capture stiction. These are the main motivations for the recent extensions of the model, see [5, 13].

For the case $\alpha = 1$ the Dahl model (10) becomes

$$\frac{dF}{dt} = \sigma v - \frac{F}{F_c}|v|.$$

Introducing $F = \sigma z$ the model can be written as

$$\begin{aligned} \frac{dz}{dt} &= v - \frac{\sigma|v|}{F_c}z, \\ F &= \sigma z. \end{aligned} \tag{11}$$

The Bristle Model

Haessig and Friedland introduced a friction model in [28], which attempted to capture the behavior of the microscopical contact points between two surfaces.

Due to irregularities in the surfaces the number of contact points and their location are random. Each point of contact is thought of as a bond between flexible bristles. As the surfaces move relative to each other the strain in the bond increases and the bristles act as springs giving rise to a friction force. The force is then given by

$$F = \sum_{i=1}^{N} \sigma_0 (x_i - b_i) \tag{12}$$

where N is the number of bristles, σ_0 the stiffness of the bristles, x_i the relative position of the bristles, and b_i the location where the bond was formed. As $|x_i - b_i|$ equals δ_s the bond snaps and a new one is formed at a random location relative to the previous location.

The complexity of the model increases with N. Good results were found with 20–25 bristles, but even a single bristle gave reasonable qualitative behavior. The stiffness of the bristles, σ_0, can be made velocity dependent. An interesting property of the model is that it captures the random nature of friction. The randomness depends on the number of bristles. The model is inefficient in simulations due to its complexity. Motion in sticking may be oscillatory since there is no damping of the bristles in the model.

The Reset Integrator Model

Haessig and Friedland also proposed the reset integrator model in the same article [28]. This model can be viewed as an attempt to make the bristle model computationally feasible. Instead of snapping a bristle the bond is kept constant by shutting off the increase of the strain at the point of rupture. The model utilizes an extra state to determine the strain in the bond, which is modeled by

$$\frac{dz}{dt} = \begin{cases} 0 & \text{if } (v > 0 \text{ and } z \geq z_0) \text{ or } (v < 0 \text{ and } z \leq -z_0) \\ v & \text{otherwise} \end{cases}$$

The friction force is given by

$$F = (1 + a(z))\sigma_0(v)z + \sigma_1 \frac{dz}{dt} \tag{13}$$

where $\sigma_1 dz/dt$ is a damping term that is active only when sticking. The damping coefficient can be chosen to give a desired relative damping of the resulting

spring-mass-damper system. Stiction is achieved by the function $a(z)$, which is given by

$$a(z) = \begin{cases} a & \text{if } |z| < z_0 \\ 0 & \text{otherwise} \end{cases} \tag{14}$$

If $|z| < z_0$ the model describes sticking where the friction force is a function of z. As the deflection reaches its maximum value z_0, the variable z remains constant and the friction force drops since $a(z)$ becomes zero. The friction force when slipping is an arbitrary function of the velocity given by $\sigma_0(v)$. The reset integrator model is far more efficient to simulate than the bristle model, but it is discontinuous in z, and detection of $|z| > z_0$ is necessary.

The Models by Bliman and Sorine

Bliman and Sorine have developed a family of dynamic models in a series of papers [6, 7, 8]. It is based on the experimental investigations by Rabinowicz, see [44].

Bliman and Sorine stress rate independence. The magnitude of the friction depends only on $\operatorname{sgn} v$ and the space variable s defined by

$$s = \int_0^t |v(\tau)| d\tau .$$

In the Bliman-Sorine models, friction is then a function of the path only. It does not depend on how fast the system moves along the path. This makes it possible to use the elegant theory of hysteresis operators developed in [35, 54]. The models are expressed as linear systems in the space variable s.

$$\begin{aligned} \frac{dx_s}{ds} &= Ax_s + Bv_s \\ F &= Cx_s \end{aligned} \tag{15}$$

The variable $v_s = \operatorname{sgn}(v)$ is required to obtain the correct sign. Bliman and Sorine have models of different complexity. The first order model is given by

$$A = -1/\varepsilon_f, \quad B = f_1/\varepsilon_f \quad \text{and} \quad C = 1. \tag{16}$$

This model can be written as

$$\frac{dF}{dt} = \frac{dF}{ds}\frac{ds}{dt} = |v|\frac{dF}{ds} = f_1/\varepsilon_f \left(v - |v|\frac{F}{f_1} \right)$$

which is identical to the Dahl model (10) with $F_C = f_1$, $\sigma = f_1/\varepsilon_f$ and $\alpha = 1$. The first order model does not give stiction, nor does it give a friction peak at a specific break-away distance as observed by Rabinowicz. This can, however, be achieved by a second order model with

$$\begin{aligned} A &= \begin{pmatrix} -1/(\eta\varepsilon_f) & 0 \\ 0 & -1/\varepsilon_f \end{pmatrix}, \\ B &= \begin{pmatrix} f_1/(\eta\varepsilon_f) \\ -f_2/\varepsilon_f \end{pmatrix} \text{and} \quad C = \begin{pmatrix} 1 & 1 \end{pmatrix}, \end{aligned} \tag{17}$$

where $f_1 - f_2$ corresponds to kinetic friction reached exponentially as $s \to \infty$, see [8]. The model (17) can be viewed as a parallel connection of a fast and a slow Dahl model. The fast model has higher steady state friction than the slow model. The force from the slow model is subtracted from the fast model, which results in a stiction peak. Both the first and second order models can be shown to be dissipative. Bliman and Sorine also show that, as ε_f goes to zero, the first order model behaves as a classical Coulomb friction model, and the second order model as a classical model with Coulomb friction and stiction. It should be noted that the Stribeck effect of the second order model, claimed by the authors, is not the same as observed in [52]. The emulated effect by the second order model is only present at a certain distance after motion starts. This means that it will not appear when the motion slows down, as the true Stribeck effect would. The friction peak is instead the equivalent of stiction for a dynamic model.

Models for Lubricated Contacts

The friction interfaces in most engineering applications are lubricated. Friction models have therefore been derived using hydrodynamics. Viscous friction is a simple example, but other models also exist. In [29] a model based on the hydrodynamics of a lubricated journal bearing is introduced. The model stresses the dynamics of the friction force. The eccentricity ε of the bearing is an important variable in determining the friction force. A simplified model is given by

$$F = K_1(\varepsilon - \varepsilon_{tr})^2\Delta + \frac{K_2}{\sqrt{1-\varepsilon^2}}v. \tag{18}$$

The first term is due to the shearing of the asperity contacts and the second term is due to the viscosity of the lubricant. The function Δ is an indicator function that is one for $\varepsilon > \varepsilon_{tr}$ and zero otherwise. This implies that for small eccentricities there is no friction due to asperity contacts. The eccentricity is given by a fourth-order differential equation, which determines the pressure distribution in the

lubricant. The model requires five parameters. Simulations show a behavior very similar to the observations in [31]. An extension including sleeve compliance is given in [30]. The model then becomes even more complicated and requires determination of initial values when switching between slipping and sticking.

The LuGre Model

The LuGre model is a dynamic friction model presented in [13]. Exstensive analysis of the model and its application can be found in [39]. The model is related to the bristle interpretation of friction as in [28]. Friction is modeled as the average deflection force of elastic springs. When a tangential force is applied the bristles will deflect like springs. If the deflection is sufficiently large the bristles start to slip. The average bristle deflection for a steady state motion is determined by the velocity. It is lower at low velocities, which implies that the steady state deflection decreases with increasing velocity. This models the phenomenon that the surfaces are pushed apart by the lubricant, and models the Stribeck effect. The model also includes rate dependent friction phenomena such as varying break-away force and frictional lag. The model has the form

$$\begin{aligned} \frac{dz}{dt} &= v - \sigma_0 \frac{|v|}{g(v)} z, \\ F &= \sigma_0 z + \sigma_1(v)\frac{dz}{dt} + f(v), \end{aligned}$$

where z denotes the average bristle deflection. The model behaves like a spring for small displacements. Linearization of (4) around zero velocity and zero state gives

$$\begin{aligned} \frac{d(\delta z)}{dt} &= \delta v, \\ \delta F &= \sigma_0 \delta z + (\sigma_1(0) + f'(0))\delta v. \end{aligned}$$

The parameter σ_0 is the stiffness of the bristles, and $\sigma_1(v)$ the damping. For constant velocity the steady state friction force is

$$F = g(v)\,\mathrm{sgn}(v) + f(v). \tag{19}$$

The function $g(v)$ models the Stribeck effect, and $f(v)$ is the viscous friction. A reasonable choice of $g(v)$ which gives a good approximation of the Stribeck effect is

$$g(v) = \alpha_0 + \alpha_1 e^{-(v/v_0)^2}, \tag{20}$$

compare with (6). The sum $\alpha_0 + \alpha_1$ then corresponds to stiction force and α_0 to Coulomb friction force. The parameter v_0 determines how $g(v)$ vary within its bounds $\alpha_0 < g(v) \leq \alpha_0 + \alpha_1$. A common choice of $f(v)$ is linear viscous friction $f(v) = \alpha_2 v$ as in (2), see also (3).

The following special case of the model given by Equations (4) and (20), which has linear viscous friction and constant σ_1, is called the *standard parameterization*.

$$\begin{aligned} \frac{dz}{dt} &= v - \sigma_0 \frac{|v|}{g(v)} z \\ g(v) &= \alpha_0 + \alpha_1 e^{-(v/v_0)^2} \\ F &= \sigma_0 z + \sigma_1 \dot{z} + \alpha_2 v \end{aligned} \tag{21}$$

It is useful to let the damping σ_1 decrease with increasing velocity, e.g.

$$\sigma_1(v) = \sigma_1 e^{-(v/v_d)^2}. \tag{22}$$

Physically this is motivated by the change of the damping characteristics as velocity increases, due to more lubricant being forced into the interface. Another reason for using (22) is that it gives a model which is dissipative, see [39].

5. Comparison of the Bliman-Sorine and the LuGre Models

The Bliman-Sorine (15) and the LuGre models (21) are both extensions of the Dahl model (10). The Dahl model (10) has many attractive features. It is a dynamic model that captures many aspects of friction. The model is so simple that it can be used for model based friction compensation. It has, however, a serious drawback because it does not describe stiction. The Bliman-Sorine and the LuGre models attempt to also capture the stiction phenomenon. Bliman and Sorine use two Dahl models in parallel to model stiction. The LuGre model captures stiction by introducing a velocity varying coefficient. The models have many similarities but also significant differences, which will be discussed in this section.

Rate dependency

The LuGre model is inherently rate dependent. The Bliman-Sorine model is seemingly independent of rate because it is expressed in terms of the space

variable s. There are, however, some subtleties because the term $v_s = \operatorname{sgn} v(t)$ enters the right hand side of Equation (15). The variable v_s which takes the values 1 or -1 changes sign when the velocity changes sign. This introduces a special kind of time dependency in the model, because there will be a transient when the velocity changes sign. After the transient the friction will settle to the steady state solution of Equation (15), which is given by

$$F^\circ = -CA^{-1}Bv_s. \tag{23}$$

The transient which makes F different from F° is the mechanism that give rise to stiction. The shape of the transient, and therefore the friction characteristics of the model, is dependent on if the velocity reversal takes place from a steady state or not. As a result the transient will cause difficulties when there are rapid changes of sign of the velocity.

The ideal model trajectory going from steady state for $-v_s$ to steady state for v_s without sign reversal in velocity is written

$$F^*(s, v_s) = Ce^{As}\left(A^{-1} + \int_0^s e^{-A\sigma}d\sigma\right)Bv_s. \tag{24}$$

This trajectory is also defined by the unique solution $x_s(0) = -F^\circ$ of

$$\max_{x_s(0),\, s} F(s), \tag{25}$$

for constant v_s, i.e. (24) is the trajectory giving the largest break-away friction force. Consequently trajectories that do not start from steady state for $s = 0$ give different friction characteristics than F^*. For example model trajectories starting with zero states give a stiction peak $f_s - f_k$ only half that of $F^*(s)$.

Oscillatory Behavior at Low Velocities

A simple experiment that reveals much about friction is to explore the open loop behavior of a drive system. Let J be the moment of inertia, F the friction torque, and u an external driving torque. The system is described by

$$J\frac{d^2x}{dt^2} + F = u. \tag{26}$$

Figures 7 and 8 show the responses to a sinusoidal input torque $u = 0.4\sin(t)$ [Nm] for the Bliman-Sorine and the LuGre models.

With the Bliman-Sorine model shown in Figure 7 there are significant oscillations in the friction force in the stick mode. Because of the oscillations the friction force F differ from F^* given by Equation (24). One effect of this is that the break-away force becomes difficult to predict. As noted above the zero initial conditions used in the simulation result in a smaller first stiction peak, resulting in a remaining bias in position. In degenerate cases with non-steady state initial conditions and oscillatory behavior a symmetric periodic input force can give a unidirectional stick-slip motion.

With the LuGre model shown in Figure 8 there are rapid changes in the friction force which brings the system quickly to rest. Compare [14] for a detailed discussion. There are, however, no oscillations in the friction force and no remaining bias in the displacement. All stiction peaks are of the same magnitude.

The oscillatory behavior of the Bliman-Sorine model is further illustrated in Figure 9, which shows the phase plane. The friction torque $F = x_1+x_2$ is shown in the Figure. We also show the trajectory that would be obtained with the friction F^*. Note that the oscillations force the trajectory of F inside the trajectory of F^*, resulting in a lower friction torque in the transient. The behavior shown in Figure 7 is clearly not desirable.

Damping

Insight into the differences between the models illustrated in Figures 8 and 7 can

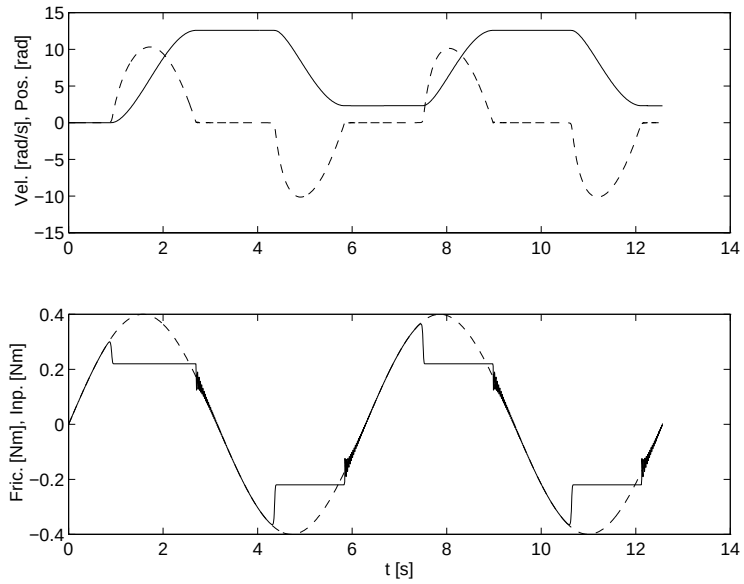

Figure 7 Response of the system (26) with Bliman-Sorine friction to a small sinusoidal disturbance torque.

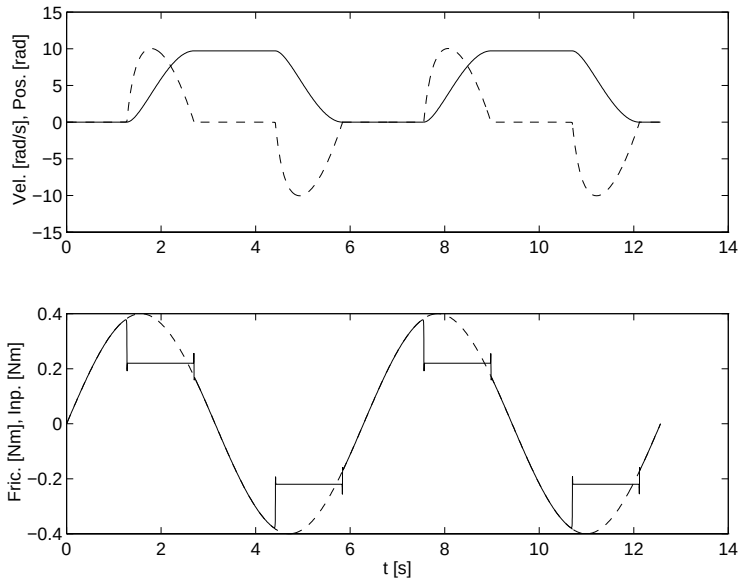

Figure 8 Response of the system (26) with LuGre friction to a small sinusoidal disturbance torque.

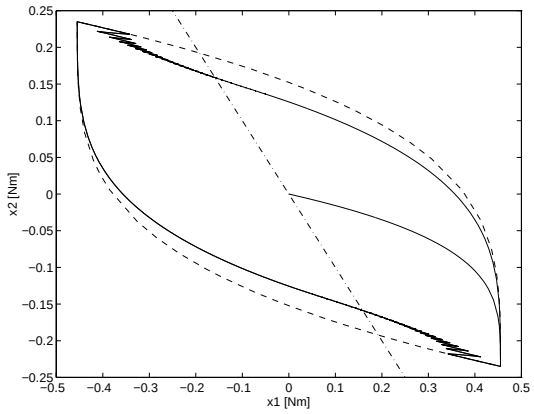

Figure 9 Phase plane corresponding to Figure 7 for the Bliman Sorine model. The ideal trajectory F^* is also shown in dashed lines. The dash-dotted line is the curve where the friction is zero.

also be obtained by linearizing the model (26) for motions with small velocity. We get

$$\frac{d^2x}{dt^2} + 2\zeta\omega\frac{dx}{dt} + \omega^2\theta = \frac{u}{J}. \tag{27}$$

The Bliman-Sorine model with linear viscous friction has the relative damping

$$\zeta = \frac{F_v}{2}\sqrt{\frac{\varepsilon_f\eta}{Jf_1 - \eta f_2}}. \tag{28}$$

The damping is thus proportional to the viscous friction coefficient F_v. This means that a low velocity property for the stick region is determined entirely

by a high velocity property in slip, and cannot be chosen freely. The relative damping for the LuGre model is

$$\zeta = \frac{\sigma_1 + \alpha_2}{2\sqrt{J\sigma_0}}, \tag{29}$$

The damping thus depend on the parameter σ_1 which can be chosen freely independent of the viscous friction coefficient α_2.

Dissipativity

Dissipativity is a very desirable property of a friction model. The Bliman-Sorine model is dissipative. The LuGre model is dissipative if

$$\sigma_1 < 4\frac{g(v)}{|v|} \tag{30}$$

This indicates that it is highly desirable that the damping coefficient σ_1 is velocity dependent. A possible choice is (22).

Behavior for Small Displacements

The behavior for small displacements is of particularly interest for control, particular in applications that involve precision pointing or positioning. For small displacements the system operates in a region where the friction force changes very rapidly.

An experiment that reveals much about the behavior at small displacements is to apply an input force $T = b + a\sin\omega t$ to the system described by Equation (26). It is interesting to have a close to b so that the velocity will be small for a long period. This can be enhanced by choosing waveforms where the force is close to zero for even longer periods. It is interesting to separate the case when $b \geq a$, which implies that the force is unidirectional, from $b < a$ when there may be velocity reversals. The behavior is very different in these cases. The behavior obtained with the different friction models are also quite different.

Early experiments of this type are described in [17]. Similar experiments with servo drives were described in [11]. The data in this section are from [25]. They were obtained from experiments with a DC-servo with a gear box. The servo drive is well lubricated. A mechanical brake was used to increase dry friction. It is easy to perform experiments with a unidirectional torque, i.e. $b \geq a$. Because of the gear box it is difficult to make meaningful experiments with a torque that changes sign because the backlash in the gear box may hide the friction effects.

Figure 10 shows the responses. The behaviors are similar for small input torques, when typical hysteresis motion is exhibited. The behavior changes with increasing torque level. For larger input torques, the behavior is elastic when dry friction dominates and plastic in the in the lubricated case. In both cases the elastic stiffness changes rapidly at certain displacements. The Bliman-Sorine

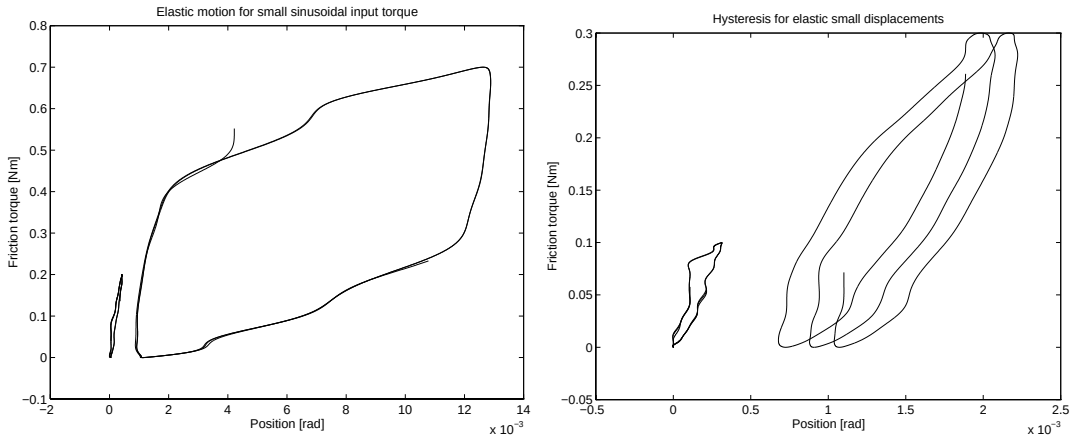

Figure 10 Results of experiments with a sinusoidal torque $T = b + a \sin t$. Dry friction dominates in the curves on the left where a brake is applied. The parameters are $a = b = 0.05$ Nm for the small hysteresis loop and $a = b = 0.35$ for the large loop. Lubricated friction dominates in the figure on the right where the parameters are $a = b = 0.10$ Nm for the small hysteresis loop and and $a = b = 0.15$ Nm for the large loop.

and the LuGre models do not separate between the cases when dry friction or viscous friction dominates. These cases only differ in terms of the values of the coefficients. Simulations of the experiment were carried out for both models. The results are shown in Figure 11. The friction models parameters are the result of identification on the servo. The LuGre identification procedure results in model parameters adapted to the large initial stiffness of the servo, whereas the Bliman-Sorine model identification gives parameters adapted to the overall presliding stiffness. As a consequence the LuGre model underestimates the displacements in the simulations. The model responses differ significantly from the experimental results. This behavior will not change substantially if the parameters are changed. The models do not succeed in reproducing the behavior with a hysteresis loop with slip found in the experiment. See [26] for an extension of the LuGre model to approach to this problem, and [20] for a correction of the Dahl model.

Notice, however, that both models gives the correct qualitative behavior for experiments where the perturbations torque changes sign. This is illustrated for

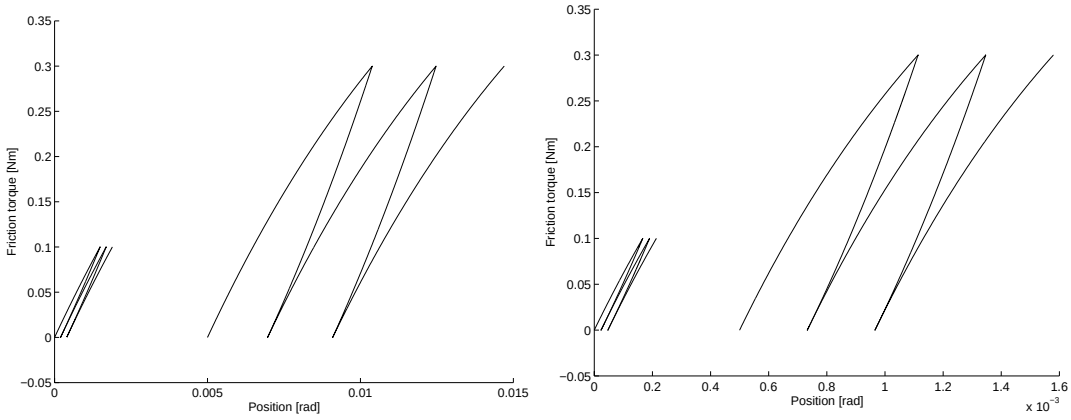

Figure 11 Simulation of the experiment in Figure 10 with the Bliman-Sorine model (left) and the LuGre model (right). The parameters are $a = b = 0.05$ Nm for the small hysteresis curve and $a = b = 0.15$ Nm for the large hysteresis curve.

the LuGre model in the Figure 12, which shows simulations for the case $b < a$. Notice that closed hysteresis loops occur in both cases and that there is slip in the case $b \neq 0$. This observation may provide useful hints for modification of the model.

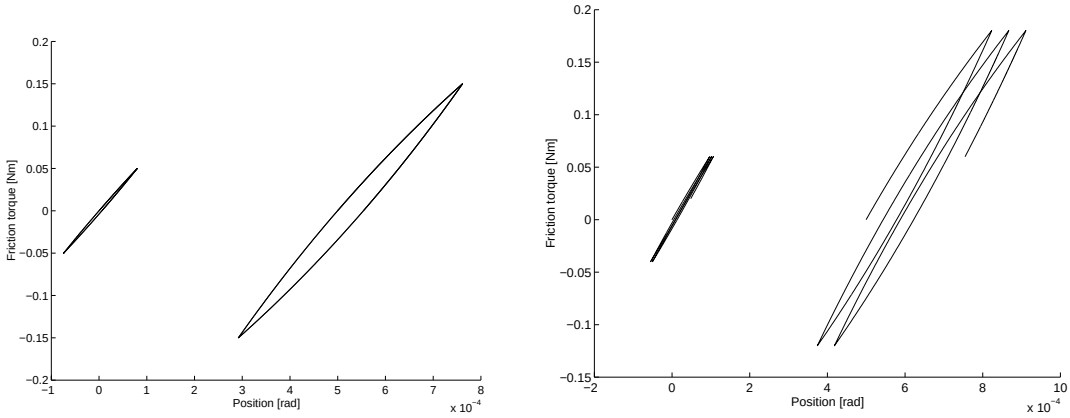

Figure 12 Simulation of experiments with perturbation torques that change sign with the LuGre model. In the left Figure the parameters are $a = 0.05$ Nm, $b = 0$ Nm for the small hysteresis loop and $a = 0.15$ Nm, $b = 0$ Nm for the large hysteresis loop. In the right Figure the parameters are $a = 0.05$ Nm, $b = 0.01$ Nm for the small hysteresis loop and $a = 0.15$ Nm, $b = 0.3$ Nm for the large hysteresis loop.

6. Control Systems Applications

In control engineering it is of interest to model systems with friction to better understand their behavior and to design control strategies that can alleviate the

performance deterioration due to friction. This is of interest in simple devices such as standard process control loops with valves and in complicated precision systems for accurate pointing, for example telescopes, radars, robots and gun turrets.

Friction Compensation

There are many ways to compensate for friction. A very simple way to eliminate some effects of friction is to use a dither signal, that is a high frequency signal that is added to the control signal. An interesting form of this was used in gyroscopes for auto pilots in the 1940s. There the dither signal was obtained simply by a mechanical vibrator, see [41]. The effect of the dither is that it introduces extra forces that makes the system move before the stiction level is reached. The effect is thus similar to removing the stiction. A modern version is the Knocker, introduced in [32], for use in industrial valves. The effects of dither in systems with dynamic friction (LuGre) was recently studied in [43].

Systems for motion control typically have a cascade structure with a current loop, a velocity loop and a position loop. Since friction appears in the inner loop it would be advantageous to introduce friction compensation in that loop. This is difficult to do with conventional systems because it is not easy to modify the current loop. Because of the price and performance of micro electronics there is a trend that current loops are implemented with computer control. With such implementations it is natural to make the friction compensation in the inner loop.

To obtain an effective friction compensation it is necessary that the velocity is measured or estimated with good resolution and small time delay. Friction compensation is more difficult if there is considerable dynamics between the control signal and the friction force. The sensor problem can be considerable with a shaft encoder because there will be a variable delay in estimation of the velocity.

If a good friction model is available it is possible to use a model based friction compensation scheme. The idea is very simple. The friction force F is estimated using some model, and a signal that compensates the estimated friction force $\hat{F}$ is added to the control signal. This is illustrated in the block diagram in Figure 6.

For tracking tasks friction can be predicted and partially compensated by feedforward. This has the advantage of eliminating the lag and the noise effects of the velocity prediction. It is only suitable for tracking since the desired velocity trajectory is known in advance.

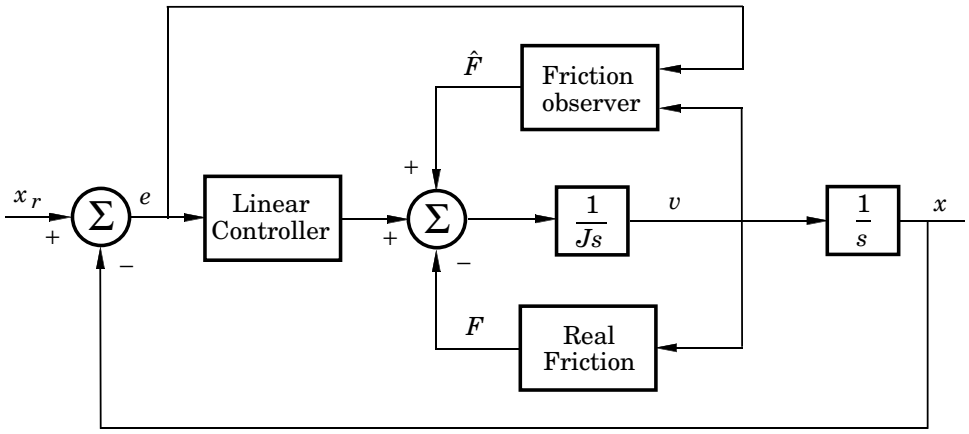

Figure 13 Block diagram of the observer-based friction compensation scheme.

An early application to an optical telescopic drive is presented in [27]. A model reference adaptive system was designed based on Coulomb. The paper [11] describes an application to velocity control. A static friction model with Coulomb and viscous friction is used. The model allows for asymmetric friction characteristics. The measurement of the velocity is critical. It is also useful not to overcompensate the friction, since this may lead to instabilities. The system has been used extensively in the control laboratory. It requires occasional adjustments of the friction parameters and gives good results. Schemes of this type are now standard in motion control systems. The performance of the friction compensation can be improved by using more elaborate friction models and by adapting their parameters.

A friction compensator for a position servo with velocity and position control based on the LuGre model is described in [13]. The design is based on passivity. It is shown that the system can be decomposed into a standard feedback configuration with a linear block and a nonlinear block. Passivity theory is used to derive conditions on the controller that guarantees that the closed loop system is stable. The condition is that the resulting linear block is SPR. In [39] and [40] it is shown that it is sufficient to have a linear block that is PR. This is very important from a practical point of view because it applies to the case where there is integral action in the inner loop. The LuGre model has also been used in connection with more complex nonlinear systems, such as robot manipulators. In this case the parameterization (22), which renders the friction model passive for all velocities, can be used explicitly in the design of passivity-based tracking controllers for n-DOF rigid robots [22]. In this context, passivity is used to generalize the SPR condition of the upper-block linear operator in [13].

Another approach to friction compensation using the LuGre model is pre-

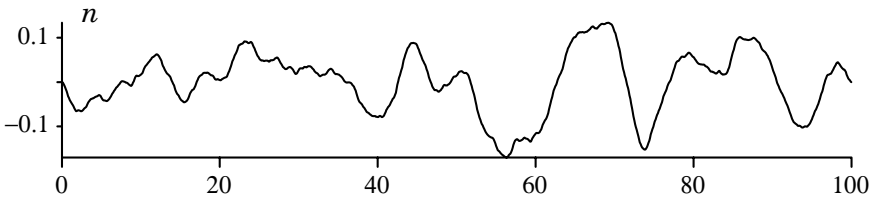

Figure 14 Velocity disturbance for the servo problem.

sented in [42]. Global tracking of a n-dof robot manipulator is ensured using only measurements of position and velocity, with all system parameters (robot and friction model) unknown. This is acheived with an adaptive controller that dominates the effects of friction (in a suitable Lyapunov function derivative) with a function of the measured signals. The controller is non-smooth, but the stabilization does not rely on the generation of sliding regimes.

The Bliman and Sorin LSI model can also be used for friction compensation. The main difference is that the control design is realized directly in the spatial coordinates instead of in the time domain as with the LuGre model. The first order model (16) (which coincides with the Dahl model) has been used for friction compensation to improve the accuracy on optronic systems [51]. Applications of the Bliman-Sorine models are particularly suitable for systems with dominant elasto-plastic effects.

Velocity Tracking

Friction compensation based on the LuGre model for a servo mechanism is described in [38]. The compensation scheme is based on an observer giving an estimate of the friction. The system regarded is described by

$$\frac{dv}{dt} = u - F,$$
$$y = v + n,$$

where v is velocity, F friction and n a velocity disturbance given as band limited Gaussian noise. The control objective is to keep y close to zero in presence of the disturbance n. The realization of the disturbance used in the simulations is shown in figure 14. A linear PI controller is designed based on the linear dynamics, and a model based friction compensation is added. The control signal thus is composed of a linear and a nonlinear part $u = u_{lin} + \hat{F}$, where u_{lin} is the linear part and $\hat{F}$ is the estimated friction force. Figure 15 illustrates a simulated typical behavior of the system with the linear PI controller without friction compensation. The figure shows the tracking error, the friction torque

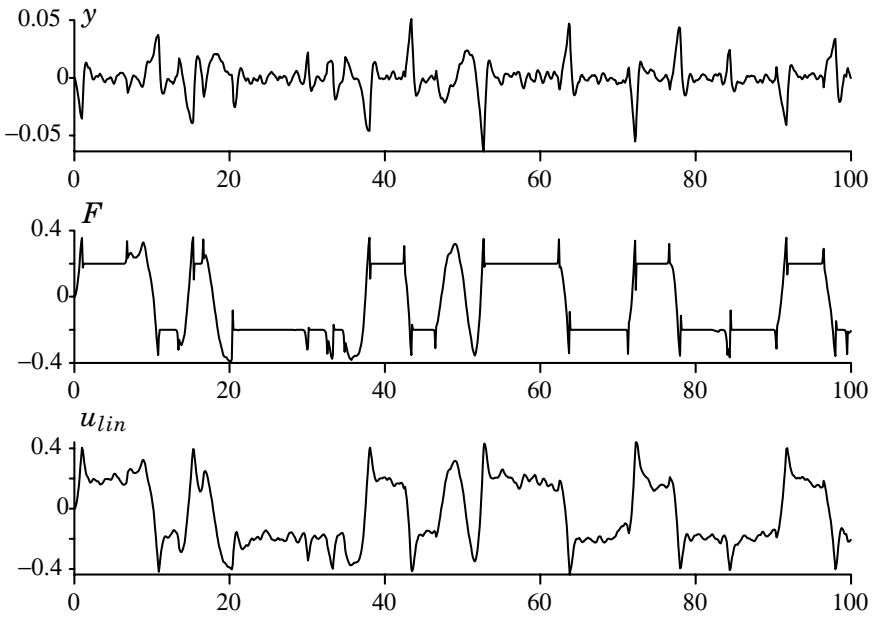

Figure 15 Illustration of performance degradation due to friction in a servo system.

and the linear control signal. Notice that there are large errors and large jumps in the control signal when the velocity passes through zero, which are due to effects of friction. An analysis of the control error shows that its distribution is far from Gaussian, with heavy tails. Also notice the rapid rise in friction force which occurs when the velocity approaches zero.

The performance improvements obtained with friction compensation based on the LuGre model are shown in Figure 16. The maximum tracking error is reduced by an order of a magnitude. Analysis of the tracking error shows that it is close to Gaussian. This observation indicates that the presence of friction can be determined from the amplitude distribution of tracking errors, provided that noise that enters the system is Gaussian. A Gaussian distribution indicates that there is no friction, deviations from the Gaussian distribution indicates that there is friction. A detailed investigation of the friction is presented in [38]. This includes comparisons with other friction models and sensitivity analysis. The measures

$$e_{rms} = \sqrt{\frac{1}{T}\int_0^T e^2(\tau)d\tau}$$

and

$$e_{max} = \max_{t\in[0,T]} |e(t)|$$

are used to evaluate the results. A summary of some results are given in table 1.

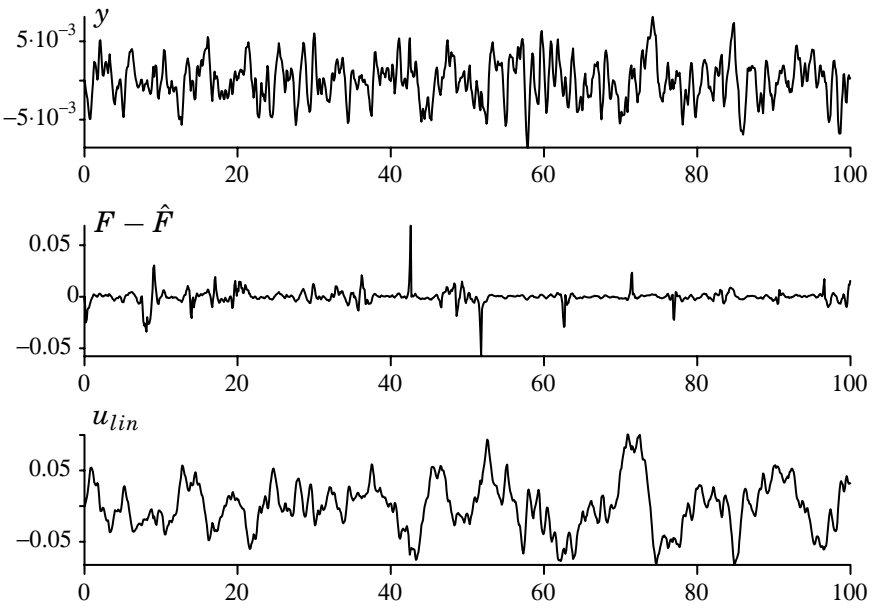

Figure 16 Behavior of the tracking system in Figure 15 when friction compensation based on the LuGre model is used.

	$e_{rms} \cdot 10^3$	$e_{max} \cdot 10^3$
No friction	3.12	9.06
With friction	13.0	63.7
Friction compensation (Coulomb)	7.85	32.7
Friction compensation (LuGre)	2.65	8.57
Overcompensation	6.72	28.5
Undercompensation	6.22	25.8

Table 1 Investigations of the effect of friction on a tracking mechanism, and the impact of some different compensation strategies.

When there is no friction the root mean square of the tracking error is $3.12 \cdot 10^{-3}$. This value increases to $13.0 \cdot 10^{-3}$ in the presence of friction. The RMS error is reduced to $7.85 \cdot 10^{-3}$ by friction compensation based on a Coulomb friction model and further to $2.65 \cdot 10^{-3}$ with a compensator based on the LuGre model. Notice that this value is smaller than the value obtained for the system without friction. The reason for this is that a PI controller was used. The dynamics of the friction observer reduces the error. In the table we also show the results when the friction force parameter in the observer is 50% too large (over-compensation) and 50% too small (under-compensation). In these cases the root mean square error increases to $6.72 \cdot 10^{-3}$ and $6.22 \cdot 10^{-3}$ respectively. The values indicate

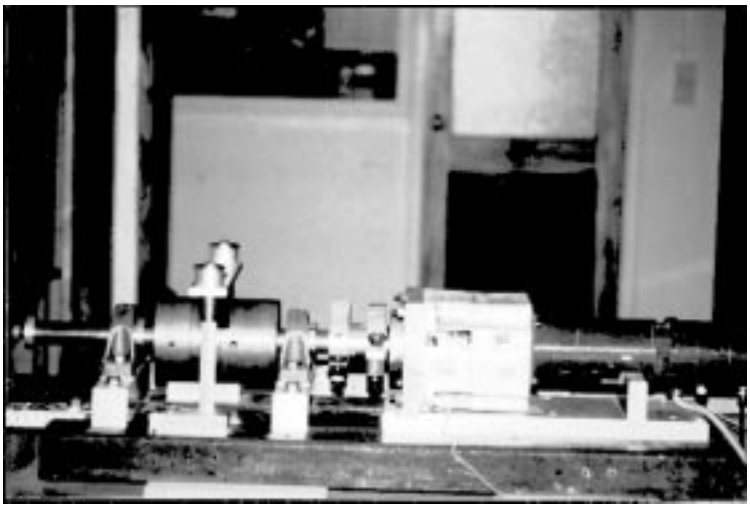

Figure 17 The test equipment used for experiments with friction compensation.

that the friction observer is not overly sensitive to parameter variations, but that there is a substantial incentive to used and adaptive scheme for friction compensation. Such a scheme will be described in the end of this section.

Laboratory Experiments

A test rig for experimenting with control of systems with friction has been built at INPG in Grenoble, see Figure 17. This equipment has a brake which makes it easy to increase friction and it is interfaced to the dSPACE signal processing equipment which makes it easy to do experiments flexible. The equipment has been used extensively for the results discussed in this paper.

The standard LuGre model (21) has been used to design friction compensators. The parameters of the model were determined by system identification experiments described in [15]. The experimental conditions were varied to emphasize different properties of the model. Experiments with “large” displacements were used to estimate the steady state friction characteristics during motion in sliding, and experiments with “small” displacements in the stiction zone were used to determine stiffness and damping. The parameter values varied with operating conditions. Some representative values are given in Table 2.

An alternative for parameter identification is proposed by Bliman and Sorine. Their idea is to determine key features of the hysteresis plot of friction force versus displacements during a cyclic motion with sign changes in velocity, typically maximum overshooting (in amplitude) and setting value (in distance). They have shown that, under certain conditions, there exists a one-to-one map between these points and the four parameters of model (17). Unfortunately, the conditions do not hold when the friction torque drops too fast after the break-

Friction parameters	Identified values
α_0	$0.28[Nm]$
α_1	$0.05[Nm]$
α_2	0.0176 [N m s/rad]
v_0	0.01 [rad/s]
σ_0	260.0 [N m/rad]
σ_1	0.6 [N m s/rad]

Table 2 Parameters of the LuGre friction model obtained from system identification. The experiments has been conducted on a DC-servo current controller (see [15]. The Complete model is $J\dot{w} = k_c u - F$, with the total inertia $J = 0.0023$ kg, and voltage/torque constant is $k_c = 1.02$ Nm/V. The friction force is F, described by the LuGre model, with the parameters given above.

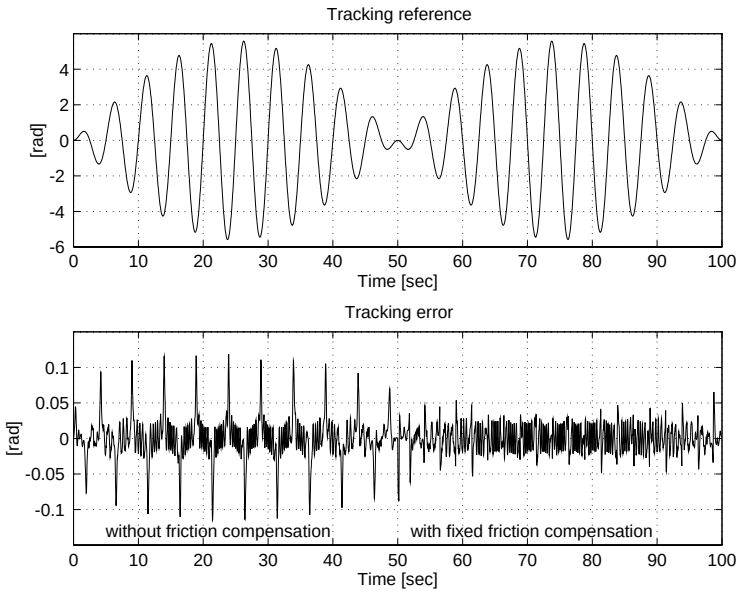

Figure 18 Tracking experiment with fixed friction compensation based on the LuGre model: reference (upper curve) and position error (lower curve).

away. This is the case for the system given by the data in Table 2.

Experimental results of friction compensation based on the LuGre model with parameters in Table 2 are shown in Figure 18. The figure shows the effects of friction which appear as large narrow peaks in the tracking error. The figure also shows the substantial improvements with friction compensation. The peaks in the tracking error practically vanishes.

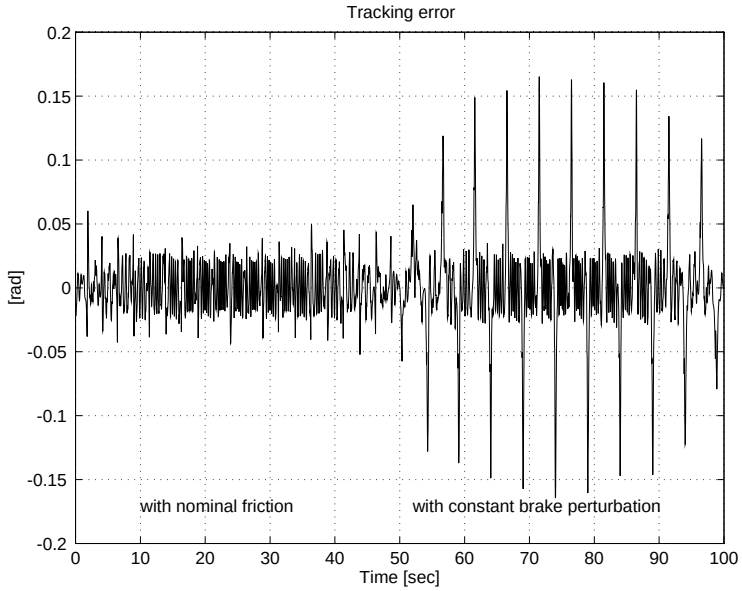

Figure 19 Tracking experiment with fixed friction compensation: position error under brake perturbation.

Friction compensation is sensitive to the friction model. This is illustrated in Figure (19), which shows data from an experiment where a mechanical brake was applied at time $t = 50$ s. The friction compensation which worked well before no longer succeeds in reducing the effects of friction. Even if this experiment exaggerates the variations in friction that occur normally it indicates the advantages of adaptive friction compensation.

Adaptive Friction Compensation.

Friction varies with many factors such as normal force, temperature, position, etc. A variation in one of these factors may change the friction characteristics in a complex manner. Since friction depends on so many factors it clearly points to the need for adaptation.

To perform adaptation we must determine which parameters in the model that should be adapted. This is a difficult problem because the parameters enter the model in a complicated way. One possibility that has been investigated is based on the model

$$\frac{dz}{dt} = v - \theta\varphi(v,x)\sigma_0\frac{|v|}{g(v)}z \tag{31}$$

$$F = \sigma_0 z + \sigma_1\dot{z} + \alpha_2 v \tag{32}$$

where θ describes the unknown parameter vector and $\varphi(v,x)$ the regressor vector. The product $\theta\varphi(v,x)$ captures variations in $1/g(v)$. It is possible to extend

the model and make the friction depend on position as well as velocity.

Adaptive observer-based friction compensation mechanisms can be designed for global asymptotic stability, see for example [**?**] and [12]. In the simplest case, only one parameter which represents the magnitude of the friction is adapted. This corresponds to $\varphi(v,x) = 1$ in Equation 32.

The main difficulty in designing adaptive mechanisms is that the variable z is not measured directly. If the inertia and the nominal friction parameters are assumed to be known, it can, however, be obtained indirectly by filtering the velocity and and the control signal. The signal

$$z_m \stackrel{\triangle}{=} \frac{1}{\sigma_1 s + \sigma_0} u - \frac{Js}{\sigma_1 s + \sigma_0} v.$$

is related to the true value of z in the following way

$$z = z_{meas} + O\left(\exp(-\sigma_0/\sigma_1 t)\right).$$

In the experiments the signal z_m is used together with the friction observer to drive the adaption by a gradient algorithm.

An advantage of adapting the parameter θ is that it is inversely proportional to the amplitude of normal forces the adaptation loop automatically gives a way to monitor the variations in the normal force.

An example from [15] is given in Figure 20. It shows that the adaptive mechanisms manages to give good tracking of the friction parameters after only a few seconds, and that it is able to cope with changes in friction. The adaptive friction compensation has also been applied to an hydraulic industrial robot, see [36].

7. Conclusions

Friction is present in many control systems for motion control. With the increase use of digital control it is now economically feasible to introduce friction compensation in such systems. This paper has shown the advantage of dynamic friction models over conventional schemes based on static friction models. Present dynamic models such as the LuGre Model and the Bliman-Sorine model are reasonably simple and they capture many but not all aspects relevant for friction compensation. Friction compensation based on these models are almost as simple as friction compensation based on static models. Many of the ad hoc fixes traditionally used, e.g. interpolation at low velocities, filtering etc., are also

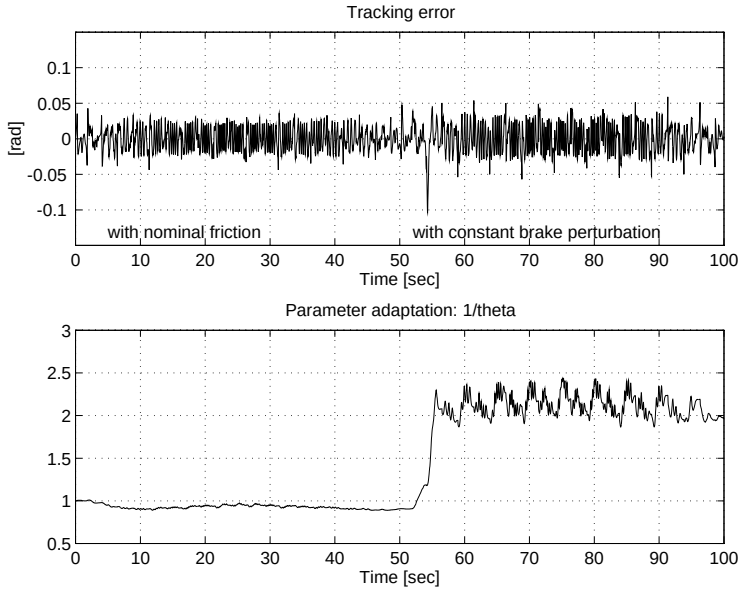

Figure 20 Tracking experiment with adaptive friction compensation: position error and estimated parameter evolution.

avoided because of the inherent dynamics in the friction model. The results are supported by simulations, experiments in the laboratory and on an industrial hydraulic robot.

8. Acknowledgements

This work has been partially supported by the Swedish Research Council for Engineering Sciences (TFR) under contract 95-759, and partially by EDF under contract P29L13/2L3074/EP663. The collaboration between Grenoble and Lund has been made under the auspices of the HCM Network ERBCHRXCT930380 on Nonlinear and Adaptive Control: Towards a design methodology for Physical Systems. This support is gratefully acknowledged.

9. References

[1] S. Andersson. Seminar at the Department of Automatic Control, Lund Institute of Technology, Lund, Sweden, 1993.

[2] B. Armstrong-Hélouvry. *Control of Machines with Friction*. Kluwer Academic Publishers, Boston, Ma., 1991.

[3] B. Armstrong-Hélouvry, P. Dupont, and C. Canudas de Wit. A survey of models, analysis tools and compensation methods for the control of machines with friction. *Automatica*, 30(7):1083–1138, 1994.

[4] C. B. Baril. *Control of Mechanical Systems Affected by Friction and Other Nondifferentiable Nonlinearities*. PhD thesis, Technion, Israel Institute of Technology, Haifa, Israel, 1993.

[5] P.-A. Bliman. Mathematical study of the Dahl's friction model. *European Journal of Mechanics. A/Solids*, 11(6):835–848, 1992.

[6] P.-A. Bliman and M. Sorine. Friction modelling by hysteresis operators. application to Dahl, sticktion and Stribeck effects. In *Proceedings of the Conference "Models of Hysteresis", Trento, Italy*, 1991.

[7] P.-A. Bliman and M. Sorine. A system-theoretic approach of systems with hysteresis. Application to friction modelling and compensation. In *Proceedings of the second European Control Conference, Groningen, The Netherlands*, pages 1844–49, 1993.

[8] P.-A. Bliman and M. Sorine. Easy-to-use realistic dry friction models for automatic control. In *Proceedings of 3rd European Control Conference, Rome, Italy*, pages 3788–3794, 1995.

[9] F.P. Bowden and D. Tabor. *The friction and Lubrication of Solids*. Oxford Univ. Press, Oxford, 1950.

[10] F.P. Bowden and D. Tabor. *The friction and Lubrication of Solids, Part II*. Oxford Univ. Press, Oxford, 1964.

[11] C. Canudas de Wit, K. J. Åström, and K. Braun. Adaptive friction compensation in DC motor drives. *IEEE Journal of Robotics and Automation*, RA-3(6):681–685, 1987.

[12] C. Canudas de Wit and P. Lischinsky. Adaptive friction compensation with partially known dynamic friction model. *Int. J. of Adaptive Control and Signal Processing*, 11(1), 1997.

[13] C. Canudas de Wit, H. Olsson, K. J. Åström, and P. Lischinsky. A new model for control of systems with friction. 40(3), 1995.

[14] C. Canudas de Wit, Henrik Olsson, Karl Johan Åström, and P. Lischinsky. Dynamic friction models and control design. In *Proceedings of the 1993*

American Control Conference, pages 1920–1926, San Francisco, California, 1993.

[15] Carlos Canudas de Wit and Pablo Lischinsky. Adaptive friction compensation with partially known dynamic friction model. *Int. Journal of Adaptive Control and Signal Processing, Special Issue on Adaptive Systems with Non-smooth Nonlinearities*, 11:65–80, 1997.

[16] J. Courtney-Pratt and E. Eisner. The effect of a tangential force on the contact of metallic bodies. In *Proceedings of the Royal Society*, volume A238, pages 529–550, 1957.

[17] J. S. Courtney-Pratt and E. Eisner. The effect of a tangential force on the contact of metallic bodies. *Proceedings of the Royal Society*, A238:pp. 529–550, 1956.

[18] P. Dahl. A solid friction model. Technical Report TOR-0158(3107–18)-1, The Aerospace Corporation, El Segundo, CA, 1968.

[19] P. Dahl. Solid friction damping of spacecraft oscillations. AIAA Paper No.75-1104 presented at the AIAA Guidance and Control Conference, Boston Mass, 1975.

[20] P. E. Dahl and R. Wilder. Math model of hysteresis in piezo-electric actuators for precision pointing systems. *Guidance and Control*, 57, 1985. AAS Paper No. AAS 885-011.

[21] Philip R. Dahl. Solid friction damping of mechanical vibrations. *AIAA Journal*, 14(12):1675–82, 1976.

[22] C. Canudas de Wit and R. Kelly. Passivity-based control design for robots with dynamic friction. In *IASTED Conference on Robotics and Manufacturing*, Cancun, Mexico, May 1996.

[23] N. Ehrich Leonard and P. Krishnaprasad. Adaptive friction compensation for bi-directional low-velocity position tracking. In *Proc. of the 31st Conference on Decision and Control*, pages 267–273, 1992.

[24] B. Friedland and Y.-J. Park. On adaptive friction compensation. In *Proceedings of the IEEE Conference on Decision and Control*, pages 2899–2902, 1991.

[25] Magnus Gäfvert. Comparison of two friction models. Master's thesis, Lund Institute of Technology, 1996.

[26] C. Ganseman, J. Swevers, and F. Al-Bender. An integrated friction model with improved presliding behaviour. In *5th IFAC Symposium on Robot Control*, Nantes, France, 1997. To appear.

[27] J. Gilbart and G. Winston. Adaptive compensation for an optical tracking telescope. *Automatica*, 10:125–131, 1974.

[28] D. A. Haessig and B. Friedland. On the modelling and simulation of friction. *J Dyn Syst Meas Control Trans ASME*, 113(3):354–362, September 1991.

[29] A. Harnoy and B. Friedland. Dynamic friction model of lubricated surfaces for precise motion control. In *Preprint No. 93-TC-1D-2*. Society of Tribologists and Lubrication Engineers, 1993.

[30] A. Harnoy and B. Friedland. Modeling and simulation of elastic and friction forces in lubricated bearings for precise motion control. *Wear*, 172:155–165, 1994.

[31] D. P. Hess and A. Soom. Friction at a lubricated line contact operating at oscillating sliding velocities. *Journal of Tribology*, 112:147–152, 1990.

[32] Tore Hägglund. Stiction compensation in control valves. In *European Control Conference*, Brussels, Belgium, 1997. To appear.

[33] V. I. Johannes, M. A. Green, and C. A. Brockley. The role of the rate of application of the tangential force in determining the static friction coefficient. *Wear*, 24:381–385, 1973.

[34] D. Karnopp. Computer simulation of slip-stick friction in mechanical dynamic systems. *Journal of Dynamic Systems, Measurement, and Control*, 107(1):100–103, 1985.

[35] M. A. Krasnoselskij and A. V Pokrovskij. *Systems with hysteresis*. Springer, New York, 1980.

[36] Pablo A. Lischinsky. *Compensation de frottement et commande en position d'un robot hydraulique industriel*. PhD thesis, Laboratiore d'Automatique de Grenoble - ENSIEG, France.

[37] A.J. Morin. New friction experiments carried out at Metz in 1831–1833. In *Proceedings of the French Royal Academy of Sciences*, volume 4, pages 1–128, 1833.

[38] H. Olsson and K. J. Åström. Observer based friction compensation. Submitted to the 35th IEEE Conference on Decision and Control, Kobe, Japan, 1996.

[39] Henrik Olsson. *Control Systems with Friction*. PhD thesis, Lund Institute of Technology, University of Lund, 1996.

[40] Henrik Olsson and Karl Johan Åström. Observer-based friction compensation. In *Proceedings of the 35th IEEE Conference on Decision and Control*, pages 4345–4350, Kobe, Japan, December 1996.

[41] W. Oppelt. A historical review of autopilot development, research, and theory in Germany. *Journal of Dynamic Systems, Measurements, and Control*, pages 215–23, September 1976.

[42] Elena Panteley, Romeo Ortega, and Magnus Gäfvert. An adaptive friction compensator for global tracking in robot manipulators. In *5th IFAC Symposium on Robot Control*, Nantes, France, 1997. To appear.

[43] A. Pervozvanski and C. Canudas de Wit. Vibrational smoothing in systems with dynamic friction. Technical report, Laboratoire d'Automatique de Grenoble, 1997.

[44] Ernest Rabinowicz. The nature of the static and kinetic coefficients of friction. *Journal of Applied Physics*, 22(11):1373–79, 1951.

[45] Ernest Rabinowicz. *Friction and wear of materials*. New York: Wiley, second edition, 1995.

[46] W. Ramberg and W. R. Osgood. Description of stress-strain curves by three parameters. Tech. Note 902, National Advisory Committee for Aeronautics, Washington, 1943.

[47] O. Reynolds. On the theory of lubrication and its application to Mr. Beauchamp Tower's experiments, including an experimental determination of the viscosity of olive oil. *Phil. Trans. Royal Soc.*, 177:157–234, 1886.

[48] R. S. H. Richardson and H. Nolle. Surface friction under time-dependent loads. *Wear*, 37(1):87–101, 1976.

[49] M. Sargin. Stress-strain relationship for concrete and the analysis of structural concrete sections. SM Study 4, Solid Mechanics Division, University of Waterloo, Canada, 1971.

[50] SKF. *General Catalogue*, 1970.

[51] M. Sorine and P. Constancis. *Mathematic Syst. Theory: the influence of R. E. Kalman*, chapter On Adaptive Solid Friction Compensation for High Accuracy Stabilization of Optronic Systems. Springer-Verlag, 1991.

[52] R. Stribeck. Die wesentlichen Eigenschaften der Gleit- und Rollenlager – The key qualities of sliding and roller bearings. *Zeitschrift des Vereines Seutscher Ingenieure*, 46(38,39):1342–48,1432–37, 1902.

[53] Nam P. Suh. *Tribophysics*. Englewood Cliffs, N.J.: Prentice-Hall, 1985.

[54] Augusto Visintin. *Differential Models of Hysteresis*. Springer, 1994.

[55] C. Walrath. Adaptive bearing friction compensation based on recent knowledge of dynamic friction. *Automatica*, 20(6):717–727, 1984.